Alginate gelation-induced cell death during laser-assisted cell printing

2014 Biofabrication 6 035022

(http://iopscience.iop.org/1758-5090/6/3/035022)

IOP Publishing Biofabrication
Biofabrication 6 (2014) 035022 (11pp) doi:10.1088/1758-5082/6/3/035022

Alginate gelation-induced cell death during laser-assisted cell printing

Hemanth Gudapati[1], Jingyuan Yan[1], Yong Huang[2] and Douglas B Chrisey[3]

[1] Department of Mechanical Engineering, Clemson University, Clemson, SC 29634, USA
[2] Department of Mechanical and Aerospace Engineering, University of Florida, Gainesville, FL 32611, USA
[3] Department of Physics and Engineering Physics, Tulane University, New Orleans, LA 70118, USA

E-mail: yongh@ufl.edu

Received 27 January 2014, revised 7 July 2014
Accepted for publication 18 July 2014
Published 14 August 2014

Abstract

Modified laser-induced forward transfer has emerged as a promising bioprinting technique. Depending on the operating conditions and cell properties, laser cell printing may cause cell injury and even death, which should be carefully elucidated for it to be a viable technology. This study has investigated the effects of alginate gelation, gelation time, alginate concentration, and laser fluence on the post-transfer cell viability of NIH 3T3 fibroblasts. Sodium alginate and calcium chloride are used as the gel precursor and gel reactant solution to form cell-laden alginate microspheres. It is found that the effects of gelation depend on the duration of gelation. Two-minute gelation is observed to increase the cell viability after 24 h incubation, mainly due to the protective cushion effect of the forming gel membrane during droplet landing. Despite the cushion effect from 10 min gelation, it is observed that the cell viability decreases after 24 h incubation because of the forming thick gel membrane that reduces nutrient and oxygen diffusion from the culture medium. In addition, the cell viability after 24 h incubation decreases as the laser fluence or alginate concentration increases.

Keywords: laser printing, cell viability, cell injury, gelation

(Some figures may appear in colour only in the online journal)

1. Introduction

Organ transplantation is limited by pathogen introduction, immune rejection, and donor shortages. Fortunately, tissue engineering provides a promising solution to the challenges associated with organ transplantation, and it aims to make need-based functional substitutes for damaged tissues and organs by directly using patient specific cells—autologous cell transfer.

Generally, tissue engineering consists of two approaches: traditional scaffold-based approach and more recent scaffold-free approach. The scaffold-based tissue engineering approach is based on seeding of cells into pre-fabricated scaffolds. Unfortunately, engineering of complex tissue constructs is still challenging using this approach because of the following reasons. Cell adhesion, migration, and proliferation into a scaffold are not effective and often difficult to control [1], and it is difficult to seed cells with the heterogeneity required to recapitulate native tissue. In addition, vascular networks required for blood circulation, nutrients supply, and waste removal *in vivo* are absent in scaffolds *in vitro* [1, 2]. The scaffold-free tissue engineering approach employs basic building blocks such as cell-laden microspheres to assemble larger functional three-dimensional (3D) tissue constructs through layer stacking, random packing, and 3D bioprinting [1, 2]. Because of its potential in scale-up automation and free form 3D positioning of different cell types, the scaffold-free approach addresses two main limitations of the scaffold-based approach: built in vascularization and controlled fabrication of complex tissue constructs [1–3]. Among various scaffold-free approaches, 3D bioprinting has emerged as one of the most promising tissue engineering approaches. 3D bioprinting is a layer-by-layer additive manufacturing technique. It takes advantage of rapid prototyping assisted by computer-aided design and/or computer-aided manufacturing procedures to build 3D tissue constructs [1].

The 3D bioprinting strategies are primarily comprised of orifice-based and orifice-free techniques. As two main orifice-based techniques, drop-on-demand (DOD) inkjetting and filamentary extrusion have been favored for biofabrication. While DOD inkjetting is good for less viscous solutions (up to 100 mPa s; such as 2% alginate solution [4]) [5, 6] to avoid possible clogging, extrusion is capable of handling much viscous solutions (even over 1000 Pa s as proposed) [5]. When DOD printing is of interest for the fabrication of high resolution, heterogeneous constructs from highly viscous biomaterials, laser-assisted 3D cell printing, mainly represented by modified laser-induced forward transfer (LIFT), provides a promising orifice-free DOD printing technique [7, 8] complementary to the orifice-based approaches such as inkjetting. Unlike inkjetting, laser-assisted cell printing is not restricted by fluid viscosity constraints because of its orifice-free dispensing approach, and it has emerged as a promising bioprinting technique [7–9]. Depending on the operating conditions and cell type, laser-assisted cell printing may cause certain cell injury and even death, which has been intensively investigated experimentally [10–12] as well as computationally [13–15]. Unfortunately, the effects of hydrogel and its gelation on cell injury and death have not been studied thus far.

The objective of this study is to investigate the effects of alginate gelation on cell death during laser-assisted cell printing. Challenges of laser-assisted cell printing include how to optimize operating conditions and material properties to mitigate cell injury. For successful realization of laser-assisted cell printing as a viable biofabrication technique, it is essential to understand and minimize process-induced cell injury and death when both cell suspension and hydrogel are printed. This study serves to investigate the effects of operating conditions such as alginate gelation, gelation time, and laser fluence as well as material properties on the post-transfer cell viability during laser-assisted cell printing. In summary, this study tests the hypothesis that the cell viability is affected by the alginate gelation process during laser-assisted cell printing and the dependence is a function of operating conditions and material properties, in particular, gelation time, laser fluence, and alginate concentration.

2. Experimental setup

2.1. Laser-assisted cell printing setup

Matrix-assisted pulsed-laser evaporation direct-write, a typical LIFT practice [7, 8, 16, 17], has been of particular interest in this study for cell printing. As shown in figure 1, the experimental setup consisted of an argon fluoride (ArF) excimer laser (Coherent ExciStar, Santa Clara, CA) with wavelength of 193 nm and 12 ns (full-width half-maximum). The laser fluence was measured using a Coherent FieldMax power/energy meter (Coherent, Portland, OR). The laser spot size diameter was maintained at 150 μm whereas the laser repetition rate was maintained at 30 Hz. The bioink was comprised of sodium alginate solution and NIH3T3 cells to

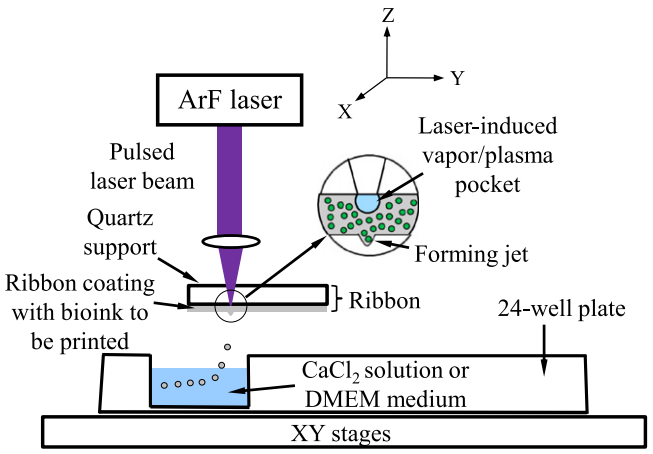

Figure 1. Schematic of laser-assisted cell printing experimental setup.

be transferred. Quartz disk (Edmund optics, Barrington, NJ) with 85% transmittance for 193 nm wavelength laser beams was used to make the ribbon, which had the bottom side coated with the bioink for bioink coating. A teflon tape (3M, St. Paul, MN) was applied on the bottom side of the quartz disk to make a 1.5×1.5 cm^2 well. Each time, 20 μL of the bioink was pipetted onto the quartz disk well and was spread evenly to produce an 80–100 μm thick layer. The receiving substrate for the transferred cells, which consisted of a substrate container and a substrate liquid, was made of a 24-well plate with one well containing either 1 ml of Dulbecco's modified Eagles medium (DMEM) or 1 ml of calcium chloride.

The laser beam, when focused onto the backside of the ribbon coating, immediately heats the coating and generates a vapor bubble at the interface of the bioink coating and the quartz disk. Subsequently, the vapor bubble expands rapidly and ejects a jet/droplet of the bioink into the receiving substrate. Ejected sodium alginate jets/droplets containing the cells were subjected to gelation when printed into the substrate container containing the calcium chloride. The droplets were not subjected to gelation when printed into the substrate container containing the DMEM culture medium. The direct writing height is the distance between the ribbon and the liquid level in substrate container and was 1 mm. The receiving substrate was mounted onto *XY* translational stages (Aerotech, Pittsburgh, PA). The ribbon and the receiving substrate moved together and the relative motion between the laser beam and the receiving substrate was set at 300 mm min^{-1} and was computer controlled.

2.2. Materials and methods

2.2.1. Bioink preparation. The bioink was comprised of sodium alginate solution and NIH 3T3 mouse fibroblast cells (ATCC, Rockville, MD). As a versatile biomaterial [18, 19], alginate hydrogel has been used as scaffolds for tissue engineering and model extracellular matrices for basic biological studies. These applications require tight control of various material properties including degradation, cell

attachment, and binding or release of bioactive molecules. Control over these properties has been achieved by chemical or physical modifications of the polysaccharide itself or the gels formed from alginate. The utility of these modified alginate gels as biomaterials has been demonstrated in a number of *in vitro* and *in vivo* studies [18] such as RGD (R: arginine; G: glycine; D: aspartic acid) modified alginate for the promotion of cell adhesion [20, 21]. Alginate, especially sodium alginate, has been frequently used as a constituent of bioink in bioprinting [3, 22, 23], to provide a structural support upon gelation. As a preliminary study, this study has used sodium alginate (NaAlg) and fibroblasts to prepare the bioink while recognizing the inert aspect of alginate.

Alginate primarily consists of a family of unbranched binary copolymers of 1,4 linked β-D-mannuronic acid (M blocks) and α-L-guluronic acid (G blocks) [24, 25]. Alginate undergoes gelation when it interacts with divalent ions such as Ca^{2+}, Ba^{2+}, Fe^{2+}, and Sr^{2+} or trivalent ions such as Al^{3+}. The gelation occurs as the cations take part in the interchain ionic binding between G-blocks in the polymer chain giving rise to a more stable 3D network [24–26]. While alginate is not an ideal material for living tissue construction, it is a good hydrogel material for proof-of-concept studies and was used in this study.

The cells were cultured in DMEM (Sigma Aldrich, St. Louis, MO) supplemented with 10% fetal bovine serum (HyClone, Logan, UT) in a humidified 5% CO_2 incubator (VWR, Radnor, PA) at 37 °C, and the culture medium was replaced every three days as required. Freshly confluent flasks of 3T3 fibroblasts were washed twice with Dulbecco's phosphate-buffered saline (Cellgro, Manassas, VA), and incubated with 0.25% Trypsin/EDTA (Sigma Aldrich, St. Louis, MO) for 5 min at 37 °C to detach the cells from the culture flasks. Then the cell suspension was centrifuged at 1000 rpm for 5 min at room temperature, and the resulting pellet was resuspended in DMEM complete cell culture medium. The re-suspended cells were adjusted to the cell concentration of 1×10^7 cells ml^{-1}.

Three different concentrations of sodium alginate solution were used in the study. Sodium alginate powder (Sigma-Aldrich, St. Louis, MO) was mixed with DMEM culture medium to obtain 2%, 4%, and 6% (w/v) of sodium alginate solution respectively. Each concentration of sodium alginate solution was mixed with NIH3T3 cells at a 50-50 percent volume ratio to obtain 1%, 2%, and 3% (w/v) of bioink with 5×10^6 cells ml^{-1}.

2.2.2. Receiving substrate preparation. A 24-well plate containing either DMEM culture medium or calcium chloride solution was used as the receiving substrate. Calcium chloride dihydrate (Sigma-Aldrich, St. Louis, MO) was used for making 2% (w/v) calcium chloride solution. A single well of the well plate was filled with either 1 ml of calcium chloride or 1 ml of DMEM culture medium and was used as the receiving substrate for the printed bioink jets/droplets. During the printing process, alginate jets/droplets underwent gelation during the impact with calcium chloride solution. The gelation occurs due to the exchange of calcium and sodium cations.

Table 1. Experimental design.

Setup	A	B
NaAlg concentration (w/v)	1%	1%, 2%, 3%
Laser fluence (mJ cm^{-2})	800, 1200, 1600	800
Gelation time (min)	2, 10	2
Cell concentration (cells ml^{-1})	5×10^6	
Receiving substrate	2% (w v^{-1}) $CaCl_2$ (gelation), DMEM medium (no gelation)	
Incubation time (h)	0, 24	
Control	Cells from unprinted bioink	

2.3. Design of experiments

As shown in table 1, two experimental setups were used to assess the effects of laser-assisted printing-related operating conditions and material properties on the post-transfer cell viability. Experimental setup A was used to investigate the effects of operating conditions such as gelation, gelation time as well as laser fluence on the cell viability. Experimental setup B was used to examine the effects of sodium alginate concentration (material property) on the cell viability. Under the experimental setup A, 1% (w/v) sodium alginate with 5×10^6 cells ml^{-1} was printed under laser fluences of 800, 1200, and 1600 mJ cm^{-2}. Under the experimental setup B, three different sodium alginate concentrations were mixed with 5×10^6 cells ml^{-1} cell suspension at 1%, 2%, and 3% (w/v), respectively, and printed under a laser fluence of 800 mJ cm^{-2}. The same amount NIH 3T3 cells from the alginate bioink that were not applied onto the ribbon were subjected to no incubation and 24 h of incubation, and they were used as the control cells for non-incubated specimens and incubated specimens, respectively.

For both the setups, two receiving substrate solutions, 2% (w/v) calcium chloride solution and DMEM culture medium, were used to study the effects of gelation. Alginate jets/droplets printed into the calcium chloride solution underwent gelation whereas those printed into the DMEM medium did not undergo any gelation. For those undergoing gelation, they were gelatinized for 2 or 10 min, the duration for post-transfer alginate jets/droplets to interact with the calcium chloride solution. Two-minute gelation condition was chosen as it was the least possible time that could be achieved in this study, and 10 min gelation condition was chosen for complete gelation as the gel membrane thickness of the microspheres reaches nearly 100% of its maximum value within the first 10 min of gelation [24]. The incubation periods used were 0 h and 24 h after printing to investigate any possible reversible cell injury [10].

2.4. Evaluation of cell viability

The viability of post-transfer NIH 3T3 cells was evaluated using 0.4% trypan blue stain (Biowhittaker, Walkersville, MD). Post-transfer cell suspension and trypan blue dye were mixed first at a 50-50% volume ratio. Then the specimens were viewed using an optical microscope, and the live/dead cell assay was performed using a hemocytometer. For the cells with intact cell membrane, the blue indicator turned bright and was colorless in the presence of active enzymes, thus indicating live cells. For the cells with permeable cell membrane, the blue stain remained inside the cells, indicating dead cells. Thereafter, the live and the dead cells were counted under the microscope.

For cells subject to no gelation, the DMEM medium with printed bioink droplets was pipetted from substrate container into a centrifuge tube and centrifuged for 2 min at 1100 rpm to get the cell specimen. When 24 h incubation was needed, the solution in substrate container was pipetted into a Petri dish containing 0.5 ml DMEM medium instead of pipetting into a centrifuge tube. Then the Petri dish was incubated for 24 h in an incubator under 5% CO_2 at 37 °C. After 24 h of incubation, the cells were detached by trypsinization prior to evaluation of the viability. Although trypsinization does not skew the live/dead ratio in this 3T3 cell-based study, it is suggested to perform the trypan blue assay directly in the plate/well.

For cells subjected to gelation, the calcium chloride solution with gelled bioink microspheres was pipetted from substrate container into a centrifuge tube, and then centrifuged for 2 min at 1100 rpm. After removing the sodium or calcium chloride-based supernatant, a 0.055 M sodium citrate solution was added into the centrifuge tube to liquefy the gelled alginate microspheres containing NIH 3T3 cells for 1 min. The resulting solution inside the centrifuge tube was then centrifuged for 2 min at 1100 rpm to harvest the cell specimen. When 24 h incubation was needed, the concentrated gel was transferred out of the centrifuge tube into a petri dish containing 1.5 ml of DMEM medium and incubated for 24 h in an incubator under 5% CO_2 at 37 °C. After 24 h of incubation, the gelled droplets were liquefied and the cell viability was evaluated.

3. Experimental results and discussion

The effects of alginate gelation, laser fluence, and alginate concentration on the post-transfer cell viability during laser-assisted cell printing are studied herein. The cell viability was measured both immediately after printing and after 24 h of incubation. Since cells may be repaired rather than proliferated within the first 24 h of incubation, incubated cells are of interest in quantifying the post-transfer cell viability during cell printing. As such, the cell viability is mainly presented and discussed based on the measurements after 24 h of incubation. All presented data has been repeated three times, and the error bars represent a standard deviation of one sigma.

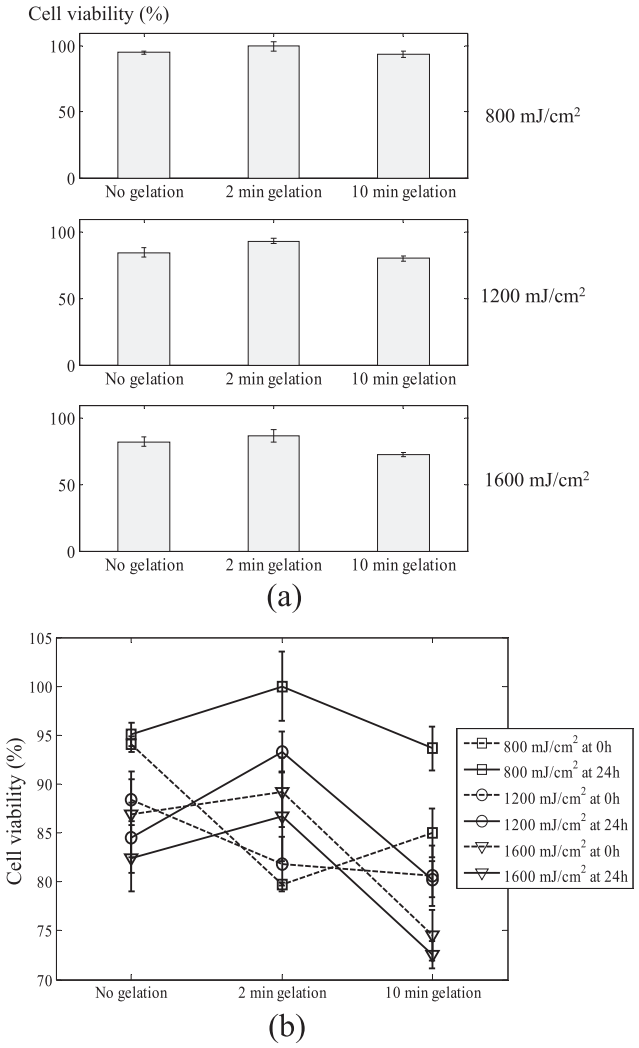

Figure 2. Effect of gelation on the cell viability measured (a) after 24 h and (b) immediately and after 24 h under different laser fluences (with the control effect considered).

3.1. Effect of gelation

As shown in figure 2, 2 min gelation increases the cell viability while 10 min gelation decreases the cell viability under the three laser fluences investigated while comparing with that under the no gelation condition (printing cells into DMEM). The higher cell viability under the 2 min gelation condition is attributed to the cushion effect [13] of a forming gel membrane. Such a membrane may effectively protect cells by minimizing detrimental mechanical stresses due to landing-induced impact [13] when alginate droplets land onto the receiving substrate. Under the no gelation case, alginate droplets don't have a protective gel membrane to minimize the introduced impact stress. However, it doesn't mean that gelation may always increase the post-transfer cell viability. Interestingly, the cell viability under the 10 min gelation condition is lower than that without gelation. This observation is attributed to the negative effect of a thick membrane on the diffusion of oxygen and nutrients. As seen from the inset of figure 3, alginate droplets are completely gelled and have no visible macro-pores. Thus, the diffusion of oxygen and

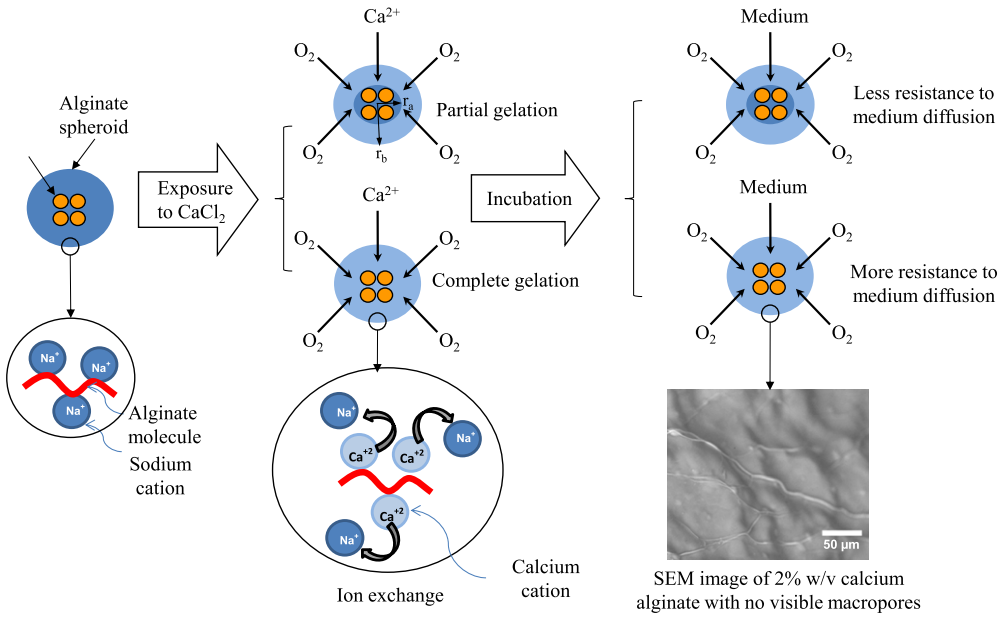

Figure 3. Alginate gelation schematic with respect to gelation time over 24 h of incubation.

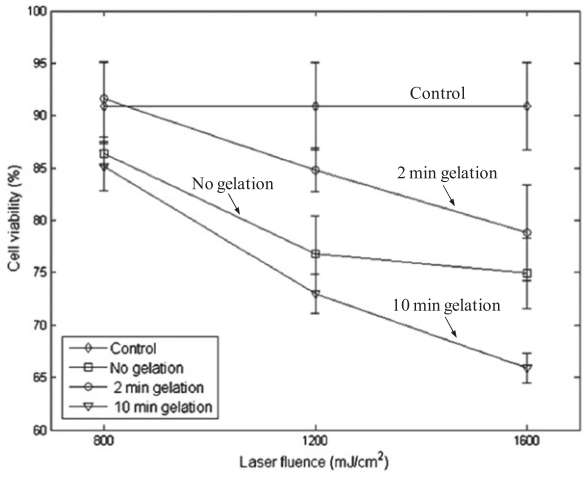

Figure 4. Effect of laser fluence on the cell viability after 24 h of incubation (without the control effect considered).

nutrients from culture medium is limited during incubation (figure 3) because of the thick gel membrane. As a result, encapsulated cells, especially injured cells, may die because of nutrient deprivation. As observed, short-duration gelation may increase the post-transfer cell viability while complete gelation may decrease the cell viability.

Moreover, the effects of gelation vary after 24 h incubation at the laser fluences investigated. Under the no gelation condition, the cell viability decreases after incubation at the three laser fluences. Under the 2 min gelation condition, the cell viability increases at both the 800 and 1200 mJ cm^{-2} laser fluences after incubation but decreases at the 1600 mJ cm^{-2} laser fluence. Under the 10 min gelation condition, the cell viability only increases at the 800 mJ cm^{-2} laser fluence after incubation and decreases at both the 1200 and 1600 mJ cm^{-2} laser fluences.

The decrease of cell viability under the no gelation condition indicates that more injured cells suffer irreversible cell injury than reversible cell injury and die because of apoptosis. The apoptotic cells are initially viewed as bright and colorless when stained with trypan blue because of their intact plasma membrane. However, after 24 h of incubation, the plasma membrane of late apoptotic cells is compromised, and these cells are viewed as blue/dead. Of course, some cells with reversible injury [10] are initially viewed as blue but become bright and colorless after 24 h of incubation since they are repaired (resealing of trivial plasma membrane damage). Overall, a decreasing trend is observed.

Cell viability under the 2 min gelation condition increases after incubation at the laser fluences of 800 and 1200 mJ cm^{-2}, indicating that during the 24 h of incubation, injured cells are able to repair the injury, including resealing their plasma membrane and restoring their intra cellular Ca^{2+} concentration to normal levels. However, the cell viability decreases at the laser fluence of 1600 mJ cm^{-2}, indicating that more cells suffer irreversible cell injury and die because of apoptosis rather than reversible cell injury at 1600 mJ cm^{-2}. The apoptotic threshold increases for cells subjected to 2 min gelation because of the cushion effect of gel membrane, resulting in more energy needed to induce apoptosis, so the cell viability drop is only observed at higher laser fluences such as 1600 mJ cm^{-2}.

Cell viability under the 10 min gelation condition increases after incubation at the 800 mJ cm^{-2} laser fluence while decreasing at the 1200 and 1600 mJ cm^{-2} laser fluences. The reason for the decrease of cell viability at the 1600 mJ cm^{-2} laser fluence and the increase of cell viability at the 800 mJ cm^{-2} laser fluence is similar to the aforementioned 2 min gelation case. However, the cell viability decreases slightly at the laser fluence of 1200 mJ cm^{-2} after incubation, indicating that the microsphere gel membrane thickness plays

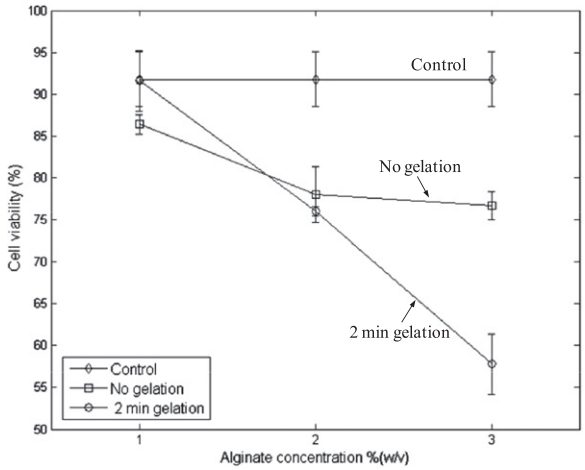

Figure 5. Effect of sodium alginate concentration on the cell viability (without the control effect considered).

an important role in determining cell death as illustrated in figure 3. Actually, the injured cell recoverability is lower under the 10 min gelation condition than that under the 2 min gelation condition. It is attributed to limited nutrient transport to encapsulated cells during incubation owing to a thick gel membrane as well as possible Ca^{2+} induced cell injury [27–30] owing to the longer exposure time of encapsulated cells to calcium chloride.

3.2. Effect of laser fluence

As seen from figure 4, the post-transfer cell viability decreases as the laser fluence increases under all investigated scenarios. Cell death is mainly due to a combined effect of process-induced mechanical normal and shear stresses/strains during jet/droplet formation [14] and landing [13, 31]. For cells subjected to gelation, the calcium ion diffusion also contributes to cell injury and even death when encapsulated cells are exposed to calcium ions although this injury plays a minor role.

For cells subjected to no gelation, the jet/droplet landing deceleration is larger at higher laser fluences, generating larger normal/shear stresses and lower cell viability [10, 11, 13]. Under the 2 min gelation and 10 min gelation conditions, gel membrane forms immediately once the jet/droplet contacts the calcium chloride solution inside the substrate container, effectively minimizing the impact of the landing-induced normal/shear stresses on the cell viability. Thus, the landing-induced cell injury does not have much influence on the cell viability for cells subjected to gelation. As observed, the cell viability under the 2 min gelation condition has higher cell viability than that of cells subjected to no gelation. However, the cell viability under the 10 min gelation condition has lower cell viability than that of cells subjected to no gelation due to limited nutrient transport to completely gelled cellular droplets during incubation as well as possible Ca^{2+} induced cell injury during 10 min gelation.

3.3. Effect of alginate concentration

The effects of sodium alginate concentration on the post-transfer cell viability are illustrated in figure 5. It can be seen that the cell viability generally decreases with the increase of sodium alginate concentration. Specially, the cell viability of the 1% sodium alginate concentration specimen is higher but the cell viability of the 2% and 3% sodium alginate concentration specimens is lower when comparing with the no gelation specimen. As aforementioned, 2 min gelation of the 1% sodium alginate specimen helps improve the cell viability by providing a protective gel membrane during landing. However, for high concentration scenarios, the forming gel membrane may have a dense gel structure, which decreases the diffusion coefficient and blocks the transport of oxygen and nutrients. As a result, the effect of protective gel membrane is overshadowed by the effect of nutrient blocking, resulting in lower cell viability for high sodium alginate concentration specimens such as 2% and 3%.

3.4. Statistical analysis

A two-sample *t*-test was used for checking the following null hypotheses: 2 min gelation time does not improve the cell viability while 10 min gelation time does not decrease the cell viability, of the encapsulated cells after 24 h incubation. The two-sample *t*-test was performed on the following sets of cell viability data at a 95% confidence interval—no gelation and 2 min gelation, no gelation and 10 min gelation, and 2 min gelation and 10 min gelation. The *p*-value of each test is less than 0.05 indicating a significant statistical difference between each of the data sets. Hence, the null hypotheses are rejected.

4. Modeling of post-transfer cell viability

4.1. Empirical modeling of post-transfer cell viability

Laser-assisted cell printing involving alginate gelation may cause cell injury and even death to post-transfer living cells. Laser printing-induced cell injury/death [11] arises because of the normal/shear stresses/strains generated during the jet/droplet formation as well as landing processes. The gelation process may alter the transmembrane (plasma membrane) ion gradients for encapsulated cells and further aggravate cell injury. In addition, gelation may affect the availability of nutrients and oxygen to encapsulated cells during incubation and also influence the cell injury reversibility.

Mathematical modeling of relationship of the cell viability dependence on the operating conditions and material properties is essential for evaluating the feasibility and efficiency of laser-assisted cell printing. However, intracellular biochemical reactions that are at the core of cell response are too complex to quantify at this stage. Alternatively, power-law [32–35], Gompertz [36–38], hybrid power-law and Gompertz [39], and statistical [40, 41] models and molecular dynamic simulations [15] have been proposed to model cell injury and/or death, including biofabrication-induced cell

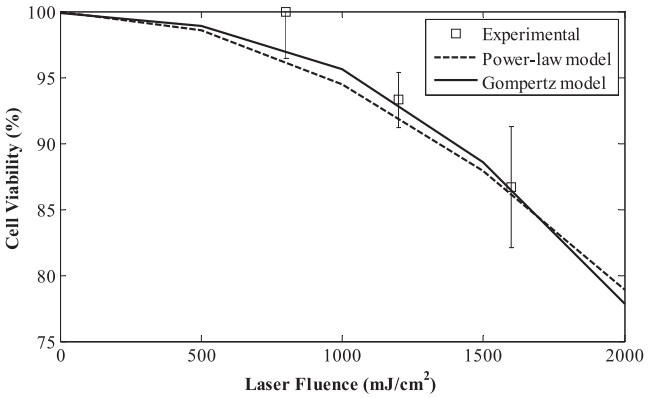

Figure 6. Cell viability as a function of varying laser fluence and 1% (w/v) constant alginate concentration for the 2 min gelation condition.

damage/death. For their simplicity, both the power-law and Gompertz models are used to model the process-induced cell injury after 24 h incubation as a preliminary study. Only the no gelation and 2 min gelation conditions are modeled since 2 min gelation appears a favorable printing condition. As a preliminary study, laser fluence and sodium alginate concentration are chosen as the inputs.

The power law cell death model used is defined as follows:

$$I = k_1 \times L^{k_2} \times A^{k_3}, \tag{1}$$

where I is the model predicted cell death in %, L is the laser fluence (mJ cm^{-2}), A is the alginate concentration, and k_1, k_2 and k_3 are the power-law model coefficients. The Gompertz cell death model is defined as follows:

$$I = \exp\left(-k_4 \exp\left(-k_5 L - k_6 A\right)\right) \times 100, \tag{2}$$

where k_4, k_5, and k_6 are Gompertz constants. To understand which model better predicts the cell viability, model prediction error is calculated and is defined as follows:

$$E = \sqrt{\frac{\sum_{i=N}^{N} \left(X_i - \bar{X}\right)^2}{N-1}}, \tag{3}$$

where $x_i = e_i - p_i$, e_i is the experimental cell viability, p_i is the model predicted cell viability, and $\bar{x}$ is the mean of x_i.

Using nonlinear least-squares data fitting with Matlab, the equation coefficients for no gelation and 2 min gelation condition are summarized in table 2. Both the simple power-law and Gompertz approaches can provide reasonable predictions for the cell viability. Overall, the power-law prediction error is 2.08 whereas the Gompertz prediction error is 2.04. For illustration, figure 6 shows the cell viability as a function of varying laser fluence for the 1% (w/v) alginate specimen under the 2 min gelation condition. As observed previously [10, 11], the cell viability decreases with the increase of laser fluence for cells subjected to gelation.

Table 2. Model coefficients.

Coefficient	Gelation condition	
	No gelation	2 min gelation
k_1 (cm^2)$^{-k2}$ (mJ)^{k2} (ml)$^{-k3}$ (g)^{k3}	0.002 054	0.068 709
k_2	1.234 831	−0.099 12
k_3	0.719 503	−0.001 43
k_4	4.436 989	12.459 07
k_5 (cm^2)$^{-1}$ (mJ)	0.000 495	0.000 728
k_6 (ml)$^{-1}$ (g)	0.179 957	0.655 481

4.2. Biophysics-based modeling approach

It should be noted that a biophysics-based modeling approach should be investigated to model the process-induced cell injury and death in future studies instead of the empirical approaches. Process-induced cell injury during laser cell printing is mainly of three types: mechanical, thermal, and chemical, and it arises because of biological damage to cells including protein damage, DNA damage, plasma membrane damage, loss of calcium ion homeostasis, accumulation of oxygen-derived free radicals, and/or metabolic energy (ATP) depletion. Cell injury is reversible up to a limit. However, beyond the limit, cell injury is irreversible and cell suffers cell death [42].

Cell death has two main types: programmed cell death and accidental cell death. Programmed cell death, represented by apoptosis, is a process by which the cell commits suicide when malfunctions arise from cell stress, cell injury, or conflicting cell division signals [43]. Programmed cell death is mediated by an intracellular genetic death program to eliminate unwanted cells, harmful cells, or cells that outlived their usefulness [44]. Apoptosis is initiated through two major pathways, at the plasma membrane by death receptor ligation (receptor or extrinsic pathway) or at the mitochondria (mitochondrial or intrinsic pathway) [45]. In contrast, accidental cell death, represented by necrosis, is due to uncontrolled injurious events. Necrosis involves rapid swelling of the cell, membrane rupture, and subsequent release of cell contents as a consequence of overwhelming physical (membrane damage, loss of ion homeostasis) or chemical (toxicity, ATP depletion) trauma to the cell. The cell death due to necrosis is a passive consequence of irreparable damage as opposed to active choice of the cell in programmed cell death [46].

During laser cell printing, laser pulses eject jets/droplets of bioink into the receiving substrate. Mechanical stresses/strains are introduced during the jet/droplet formation and landing processes. If the stresses/strains are sufficiently large, it instantaneously ruptures plasma membrane and causes cell death through necrosis. Contrastingly, if the mechanical stress is small, it does not injure the cells. However, if the mechanical stress is intermediate, it mechanically alters plasma membrane, proteins, DNA, and other organelles. The mechanical disruption of plasma membrane results in alteration of transmembrane chemical and electrical gradients, especially the calcium ion gradient when calcium chloride is

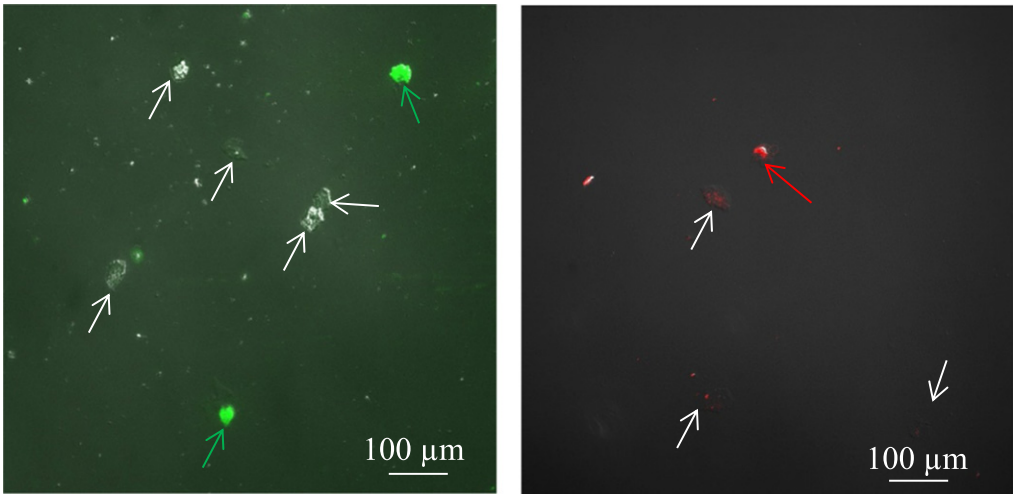

Figure 7. Post-printing apoptotic (left) and necrotic (right) 3T3 cells.

part of the receiving substrate. The alteration of transmembrane calcium ion gradient results in generation and accumulation of reactive oxygen species (ROS) in cells. In general, ROS are produced as an unavoidable by-product during metabolic energy production in cells. ROS accumulation further damages plasma membrane, proteins, DNA, and other organelles, thus triggering a vicious cycle.

Furthermore, laser energy and alginate concentration influence the morphology of cell-laden microspheres formed. The morphology of the microspheres governs the transport of nutrients and oxygen into the microspheres that consecutively governs the metabolic energy production in cells. Cell injury repair and cell death are governed by metabolic energy that is available to the cells [42, 47]. If sufficient metabolic energy is available, cell injury repair and apoptotic pathways are simultaneously activated. However, if metabolic energy is not sufficient, injured cells eventually die of necrosis. Figure 7 shows some 2 min gelation apoptotic (in green) and necrotic (in red) cells characterized by using a PromoKine apoptotic and necrotic cell detection kit (PromoCell GmbH, Heidelberg, Germany) during the printing of 1% alginate suspension with 5×10^6 cells ml^{-1} under a laser fluence of 1600 mJ cm^{-2}. Apparently, both apoptotic and necrotic cells may exist. While necrotic cells can be easily detected using a dye exclusion method, apoptotic cells must be carefully quantified over a certain period, which is of great interest in a future study. To precisely understand and model the happening of cell injury and death during laser printing, a cell death signaling pathway-based approach as shown in figure 8 is of great need as part of future work.

5. Conclusions and future work

5.1. 1 Conclusions

As a preliminary step towards understanding of cell injury and death during laser-assisted 3D cell printing, this study has investigated the effects of alginate gelation, gelation time, alginate concentration, and laser fluence on the post-transfer cell viability of NIH 3T3. Sodium alginate and calcium chloride are used as the gel precursor and gel reactant solution to form cell-laden alginate microspheres.

Some main conclusions are listed as follows. The effects of gelation depend on the duration of gelation. Two-minute gelation is observed to increase the cell viability after 24 h incubation, mainly due to the protective cushion effect of forming gel membrane during droplet landing. Despite the cushion effect from 10 min gelation, it is observed that the cell viability decreases after 24 h incubation because of the forming thick gel membrane that reduces nutrient and oxygen diffusion from culture medium. In addition, the longer exposure of encapsulated cells to calcium chloride may result in greater cell injury due to Ca^{2+} ions. As observed, the cell viability after 24 h incubation decreases as the laser fluence or alginate concentration increases.

5.2. Discussion and future work

While the fabrication of alginate droplets has been the focus of this study, the technique itself can be readily extended to fabricate 3D heterogeneous constructs. For example, 3D constructs such as a tubular alginate structure can be successfully fabricated using LIFT as illustrated in figure 9. During the printing process, the landing location for alginate droplets being deposited is the newly printed top layer of the construct being printed. The direct writing height, the distance between the ribbon and the liquid level, is set at a certain height to optimize the printing quality in terms of the feature size of deposited feature. Once deposited, the platform moves downwards to submerge into the calcium chloride solution to fully gelatinize the newly deposited alginate droplet-based layer. This process repeats until a construct is made. The relative motion between the ribbon and the receiving container as well as the platform movement can be controlled using different motion stages. In short, alginate droplets/jets are printed onto a platform which gradually lowers into a calcium chloride solution while the laser shines at a new

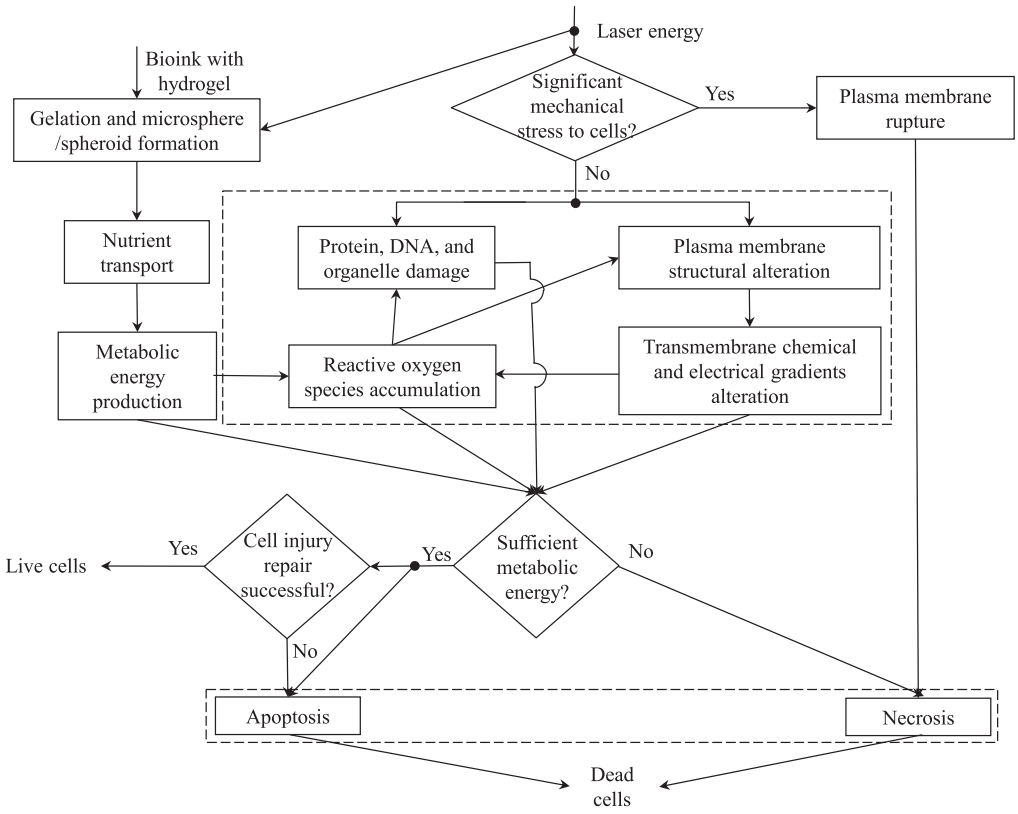

Figure 8. Cellular responses to operating conditions during laser-assisted cell printing.

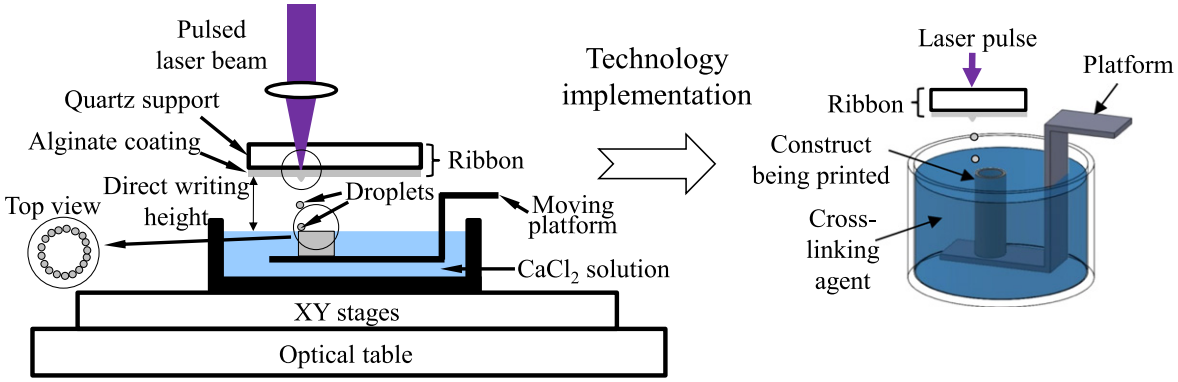

Figure 9. Schematics of laser printing-based fabrication.

ribbon location sequentially. The rate at which the platform is lowered directly corresponds to the rate at which each layer is printed, and the process can be easily automated by coordinating the motion of the platform and the ribbon.

Most available biofabrication techniques such as inkjetting and extrusion are pixel-by-pixel or line-by-line based, leading to a relatively low productivity for large constructs. Fortunately, laser printing may provide a scale-up alternative by dynamically projecting an incident laser beam using a digital mirror array, which is placed between the pulsed laser beam and the ribbon. Each mirror selectively reflects part of the incident laser beam based on the designed pattern, resulting in numerous mirror-sized sub-laser beams. Then the reflected sub-laser beams further simultaneously shine over the ribbon as the laser sources for LIFT printing. As a result, a large-scale planar pattern can be deposited as planar projection instead of pixel-by-pixel deposition.

While some empirical approaches may be able to well capture the cell injury information, the complete understanding of process-induced cell injury and death must be done with biophysics-based approaches such as the cell death signaling pathway-based approach. In addition, future studies should incorporate assays that are capable of detecting apoptosis and necrosis, especially immediately after printing, to better understand cellular responses to operating conditions. Other than the Trypan blue assay, assays capable of detecting proapoptotic proteins of the intrinsic as well as extrinsic pathways should be used to confirm whether apoptosis occurs only though the intrinsic pathway or not. Furthermore, some extra work should be devoted to improving

the process scale-up potential, in particular, laser planar projection-based printing instead of drop-wise deposition and automatic ribbon making.

Acknowledgements

The study was partially supported by the National Textile Center and the National Science Foundation (CMMI-CAREER 1321271). The authors would like to thank Ruitong Xiong, Zhengyi Zhang, Wenxuan Chai, and Jun Yin for apoptotic and necrotic cell testing.

References

[1] Guillotin B and Guillemot F 2011 Cell patterning technologies for organotypic tissue fabrication *Trends Biotechnol.* **29** 183–90
[2] Mironov V *et al* 2009 Organ printing: tissue spheroids as building blocks *Biomaterials* **30** 2164–74
[3] Xu C, Chai W, Huang Y and Markwald R R 2012 Scaffold-free inkjet printing of three-dimensional zigzag cellular tubes *Biotechnol. Bioeng.* **109** 3152–60
[4] Herran C L, Huang Y and Chai W 2012 Performance evaluation of bipolar and tripolar excitations during nozzle-jetting-based alginate microsphere fabrication *J. Micromech. Microeng.* **22** 085025
[5] Hon K K B, Li L and Hutchings I M 2008 Direct writing technology-advances and developments *CIRP Ann.—Manuf. Technol.* **57** 601–20
[6] Vaezi M, Seitz H and Yang S 2013 A review on 3D micro-additive manufacturing technologies *Int. J. Adv. Manuf. Technol.* **67** 1721–54
[7] Schiele N R *et al* 2010 Laser-based direct-write techniques for cell printing *Biofabrication* **2** 032001
[8] Riggs B C *et al* 2011 Matrix-assisted pulsed laser methods for biofabrication *MRS Bull.* **36** 1043–50
[9] Ringeisen B R *et al* 2013 Cell and organ printing turns 15: diverse research to commercial transitions *MRS Bull.* **38** 834–43
[10] Lin Y, Huang Y, Wang G, Tzeng J and Chrisey D B 2009 Effect of laser fluence on yeast cell viability in laser-assisted cell transfer *J. Appl. Phys.* **106** 043106
[11] Lin Y, Huang G, Huang Y, Tzeng T J and Chrisey D B 2010 Effect of laser fuence in laser-assisted direct writing of human colon cell *Rapid Prototyping J.* **16** 202–8
[12] Lin Y, Huang Y and Chrisey D B 2011 Metallic foil-assisted laser cell printing *Trans. ASME, J. Biomech. Eng* **133** 025001
[13] Wang W, Huang Y, Grujicic M and Chrisey D B 2008 Study of impact-induced mechanical effects in cell direct writing using smooth particle hydrodynamic method *Trans. ASME, J. Manuf. Sci. Eng.* **130** 021012
[14] Wang W, Li G and Huang Y 2009 Modeling of bubble expansion-induced cell mechanical profile in laser-assisted cell direct writing *Trans. ASME, J. Manuf. Sci. Eng.* **131** 051013
[15] Yin J and Huang Y 2011 Study of process-induced cell membrane stability in cell direct writing *Trans. ASME, J. Manuf. Sci. Eng.* **133** 054501
[16] Lin Y, Huang Y and Chrisey D B 2009 Droplet formation in matrix-assisted pulsed-laser evaporation direct writing of glycerol-water solution *J. Appl. Phys.* **105** 093111
[17] Yan J, Huang Y and Chrisey D B 2013 Laser-assisted printing of alginate long tubes and annular constructs *Biofabrication* **5** 015002
[18] Augst A D, Kong H J and Mooney D J 2006 Alginate hydrogels as biomaterials *Macromol. Biosci.* **6** 623–33
[19] Murphy S V, Skardal A and Atala A 2013 Evaluation of hydrogels for bio-printing applications *J. Biomed. Mater. Res.* A **101** 272–84
[20] Hersel U, Dahmen C and Kessler H 2003 RGD modified polymers: biomaterials for stimulated cell adhesion and beyond *Biomaterials* **24** 4385–415
[21] Sargus-Patino C 2013 Alginate hydrogel as a three-dimensional extracellular matrix for *in vitro* models of development *Master Thesis* University of Nebraska
[22] Khalil S, Nam J and Sun W 2005 Multi-nozzle deposition for construction of 3D biopolymer tissue scaffolds *Rapid Prototyping J.* **11** 9–17
[23] Nishiyama Y *et al* 2009 Development of a three-dimensional bioprinter: construction of cell supporting structures using hydrogel and state-of-the-art inkjet technology *J. Biomech. Eng.* **131** 035001
[24] Blandino A, Macías M and Cantero D 1999 Formation of calcium alginate gel capsules: influence of sodium alginate and $CaCl_2$ concentration on gelation kinetics *J. Biosci. Bioeng.* **88** 686–9
[25] Rezende R A, Bártolo P J, Mendes A and Filho R M 2007 Experimental characterisation of the alginate gelation process for rapid prototyping *Chem. Eng. Trans.* **11** 509–14
[26] Mammarella E J and Rubiolo A C 2003 Crosslinking kinetics of cation-hydrocolloid gels *Chem. Eng. J.* **94** 73–7
[27] Lee G M, Han B K, Kim J H and Palsson B O 1992 Effect of calcium chloride treatment on hybridoma cell viability and growth *Biotechnol. Lett.* **14** 891–6
[28] Martino N A *et al* 2011 Functional expression of the extracellular calcium sensing receptor (CaSR) in equine umbilical cord matrix size-sieved stem cells *PLoS One* **6** e17714
[29] McGinnis K M, Wang K K and Gnegy M E 1999 Alternations of extracellular calcium elicit selective modes of cell death and protease activation in SHSY5Y human neuroblastoma cells *J. Neurochem.* **72** 1853–63
[30] McNeil S E, Hobson S A, Nipper V and Rodland K D 1998 Functional calcium sensing receptors in rat fibroblasts are required for activation of SRC kinase and mitogen-activated protein kinase in response to extracellular calcium *J. Biol. Chem.* **273** 1114–20
[31] Wang W, Huang Y and Chrisey D B 2007 Numerical study of cell droplet and hydrogel coating impact process in cell direct writing *Trans. NAMRI/SME* **35** 217–24
[32] Blackshear P L, Dorman F D and Steinbach J H 1965 Some mechanical effects that influence haemolysis *Trans. Am. Soc. Artif. Intern. Organs* **11** 112–7
[33] Paul R *et al* 2003 Shear stress related blood damage in laminar couette flow *Artif. Organs* **27** 517–29
[34] Goubergrits L and Affeld K 2004 Numerical estimation of blood damage in artificial organs *Artif. Organs* **28** 499–507
[35] Grigioni M *et al* 2004 The power-law mathematical model for blood damage prediction: analytical developments and physical inconsistencies *Artif. Organs* **28** 467–75
[36] Reznick D N, Bryant M J, Roff D, Ghalambor C K and Ghalambor D E 2004 Effect of extrinsic mortality on the evolution of senescence in guppies *Nature* **431** 1095–9
[37] Fife J P, Ozkan H E, Derksen R C and Grewal P S 2006 Using computational fluid dynamics to predict damage of a biological pesticide during passage through a hydraulic nozzle *Biosyst. Eng.* **94** 387–96
[38] Minto C, Myers R A and Blanchard W 2008 Survival variability and population density in fish populations *Nature* **452** 344–7

[39] Li M, Tian X and Chen X 2011 Temperature effect on the shear induced cell damage in biofabrication *Artif. Organs* **35** 741–6

[40] Li M, Tian X, Zhu N, Schreyer D J and Chen X 2010 Modeling process-induced cell damage in the biodispensing process *Tissue Eng.* C **16** 533–42

[41] Li M, Tian X, Schreyer D J and Chen X 2011 Effect of needle geometry on fow rate and cell damage in the dispensing-based biofabrication process *Biotechnol. Prog.* **27** 1777–84

[42] Kumar V, Abbas A and Fausto N 2005 *Robbins & Cotran Pathologic Basis of Disease* 7th edn (Philadelphia, PA: Saunders)

[43] Fussenegger M, Bailey J E and Varner J 2000 A mathematical model of caspase function in apoptosis *Nat. Biotechnol.* **18** 768–74

[44] Engelberg-Kulka H, Amitai S, Kolodkin-Gal I and Hazan R 2006 Bacterial programmed cell death and multicellular behavior in bacteria *PLoS Genet.* **2** 1518–26

[45] Fulda S and Debatin K M 2006 Extrinsic versus intrinsic apoptosis pathways in anticancer chemotherapy *Oncogene* **25** 4798–811

[46] Henriquez M, Armisen R, Stutzin A and Quest A F 2008 Cell death by necrosis, a regulated way to go *Curr. Mol. Med.* **8** 187–206

[47] Agarwal J, Walsh A, Peters S and Lee R C 2005 Multimodal strategies for resuscitating injured cells *Ann. New York Acad. Sci.* **1066** 295–309